Analyst

Accepted Manuscript

ROYAL SOCIETY OF CHEMISTRY

www.rsc.org/analyst

Innate Immune System-Mimicking, Real-Time Biosensing of Infectious Bacteria

Sung-Min Seo[1], Jin-Woo Jeon[1], Tae-Yong Kim[1], and Se-Hwan Paek[1,2,*]

[1] Department of Bio-Microsystem Technology, Korea University, 145Anam-ro, Seongbuk-Gu, Seoul 136-701, Korea

[2] Department of Biotechnology and Bioinformatics, Korea University, 2511 Sejong-ro, Sejong 339-700, Korea

Running head: Immune system-mimicking biosensing of bacteria

[*] Address for correspondence:

Se-Hwan Paek, Professor
540 Biotechnology Building (Green Campus)
Korea University
145 Anam-ro, Seongbuk-gu
Seoul 136-701
Republic of Korea
Tel: 82-2-3290-3438
FAX: 82-2-927-2797
E-mail: shpaek@korea.ac.kr

Abstract

An animal cell-based biosensor was investigated to monitor bacterial contamination in an unattended manner by mimicking the innate immune response. The cells (RAW 264.7 cell line) were first attached on the solid surfaces of 96-well microtiter plate and co-incubated in the culture medium with a sample that might contain bacterial contaminants. As Toll-like receptors were present on the cell membrane surfaces, they acted as a sentinel by binding to pathogen-associated molecular patterns (PAMPs) of any contaminant. Such biological recognition initiates signal transmission along various pathways to produce different proinflammatory mediators, one of which, tumor necrosis factor-α (TNF-α) was measured using an immunosensor. To demonstrate automated bacterium monitoring, a capture antibody specific for TNF-α was immobilized on an optical fiber sensor tip and then used to measure complex formation in a label-free sensor system (e.g., Octet Red). The sensor response time depended significantly on the degree of agitation of the culture medium, controlling the biological recognition and further autocrine/paracrine signaling by cytokines. The response, particularly under non-agitated conditions, was also influenced by the medium volume, revealing a local gradient change of the cytokine concentration and also acidity, caused by bacterial growth near the bottom surfaces. A biosensor system retaining 50 μL medium and not employing agitation could be used for the early detection of bacterial contamination. This novel biosensing model was applied to the real-time monitoring of different bacteria, *Shigella sonnei*, *Staphylococcus aureus*, and *Listeria monocytogenes*. They (< 100 CFU/mL) could be detected automatically within the working time. Such analysis was carried out without any manual handling regardless of the bacterial species, suggesting the concept of non-targeted bacterial real-time monitoring. This technique was further applied to real sample testing (e.g., with milk) to exemplify, for example, food quality control process without using any additional sample pretreatment such as magnetic concentration.

Key words: animal cell-based biosensor, non-targeted bacterium biosensing, proinflammatory mediators, unattended real-time monitoring

Introduction

Bacterial infection of the human body can cause various diseases: as many as 76 million cases per year in United States alone, resulting in hospitalization of 325,000 people and 5,000 deaths [1]. As the invasion can be mediated via different routes, such as food intake, inhalation, and skin dermatitis [2], efficient testing techniques for the presence of the microorganisms in food products and the environments have been investigated [3]. The food industry has invested much effort, not only for screening products contaminated with specific typical pathogenic bacteria [4], but also for controlling total bacterial numbers generally below a threshold value. Nevertheless, new or mutated microorganisms can ordinarily emerge, which can affect food safety, directly affecting human health, and even increase the dangers of bioterrorism [5]. Thus, bacterial contaminations would preferably be monitored in an unattended manner and with a high sensitivity to a broad spectrum of different target organisms.

Real-time monitoring is an unattended biosensing technique that can rapidly provide analytical results for the presence of bacteria in a sample [6]. Typical examples are the continual detection of biochemical products in bacterial culture [7] or nucleic acid products via the polymerase chain reaction (PCR; [8]). Biochemistry-based detection depends on the distinct metabolisms of bacteria, resulting in different compositions of enzymes secreted into the culture medium [9]. The presence of particular enzyme(s) in the medium can be determined by colorimetric reaction(s), indicating positive or negative results. As each bacterium has a genome unique in nucleic acid sequence, amplified products, via PCR, can also be used for the identification of target microorganism [10]. This technique has further been developed to real-time monitoring of the product [11] but may be limited by the pre-cultivation required for a traceable bacterium [12]. Although real-time monitoring technologies have been developed for commercialization, multiplexed detection is limited to a small number of bacteria because the assays target selective markers linked to the analytes.

Non-targeted detection for mixed bacteria can readily be achieved using animal cells, such as macrophage and epithelial cells, which are specifically differentiated for the innate immune response of the body [13]. The cells contain cell surface receptors (e.g., Toll-like receptors; TLRs) playing the role of sentinel against external invasion by recognizing pathogen-associated molecular patterns (PAMPs; [14]). Such bindings lead to dimerization of the receptor

molecules and could offer a high affinity system for foreign entities [15]. The binding signal is transferred to the endoplasmic side of the cell, eventually activating nuclear factor-κB (NF-κB) such that transcription of genes encoding proinflammatory mediators occurs [16]. The mediators including, typically, cytokines such as tumor necrosis factor-α (TNF-α) and interleukin family members, are produced and secreted from the cells. These are propagated to neighboring cells to alert the invasion (i.e., paracrine signaling [17]) and also to activate the immune status against the stimulation, which further involves the enhancement of cell surface receptor density (i.e., autocrine signaling [18]). In the case of live bacteria, this stimulation increases in number as time goes on and, therefore, the stimulation size experienced by the host cells is also augmented. This event gradually amplifies the proinflammatory signal by synergistic interaction between grown bacteria and cellular receptors [19].

We have used the innate immune response of mammalian cells for the real-time monitoring of microbes contaminated in, for example, food, the environment, and human blood during surgery [20]. To this end, a biosensing system for bacterium was devised by incorporating a label-free immunosensor for a cytokine (e.g., TNF-α) into the animal cell (e.g., macrophage cell line; typically, RAW264.7)-grown culture that contained a test sample (Fig. 1). When the sample contained even a traceable amount of microbe, it could expand in the culture medium [20] and stimulate the cells growing on the container surfaces (Fig. 1a). The interaction between the analyte and the cell-surface receptors, TLRs, could occur and result in the production of cytokines, as mentioned above (Fig. 1b). TNF-α as a target cytokine can be detected using the capture antibody, specific to the inflammatory mediator, which was immobilized on the tip of optical fiber sensor, sensitive to mass accumulated on the sensor surfaces (Fig. 1c). Such label-free sensing enabled us to monitor in real time the cytokine concentration, for which the initial detection time will be inversely proportional to the microbial titer present in the sample medium. The detection capability can be enhanced by employing an additional antibody (the detection binder) to TNF-α, binding to the same analyte molecule together with the capture antibody in a sandwich form.

The real-time monitoring technique was characterized in this study towards performance-controlling factors during the analysis of bacterial contamination of food in an unattended manner [21]. To this end, a murine cell line, RAW264.7, originated from murine macrophages, was used as the host cell because cytokine signaling is potent relative to other cells and

human cell lines [22]. Upon infection, TNF-α is one of the cytokines produced from the cell line early and in a significant amount [23]. *Shigella sonnei* (*S. sonnei*), *Staphylococcus aureus* (*S. aureus*), and *Listeria monocytogenes* (*L. monocytogenes*), known as common contaminants [24], were selected as the infectious agents.

Materials and Methods

All reagents used in this study were of analytical grade and are listed in the Supplementary Information. Although experimental details are also described in Supplementary Information, procedures are outlined in the Results and Discussion.

Results and Discussion

Real-time Infection Monitoring using an In vitro-Innate Immune System

Secretory cytokine detection. We first tested the detection capability of the immunoassay whether it could detect TNF-α secreted from animal cells upon infection. The RAW264.7 cells were initially attached for growth on the culture container surfaces at about 50% confluency. *S. sonnei* (234±34 CFU/mL) was used to infect the animal cells placed within either the ordinary incubator or the sensor system (maintained at 36°C) with Octet Red. The microorganism and cytokine produced were determined quantitatively using a traditional colony assay technique and a commercial ELISA kit for mouse TNF-α, respectively (Fig. S1, a). The production pattern of TNF-α was close to the growth pattern of the bacterium regardless of the incubation means, indicating that the cytokine secretion was directly related to the bacterial stimulation. At the earliest stage of increase, the cytokine concentration in the culture container was approximately 1.28±0.11 ng/mL or lower, consistent with a result reported previously [20].

The TNF-α level was further detected using a label-free technique to support the analytical concept. To this end, a defined amount of cytokine was added into an identical culture container to that shown in Fig. 1 except for the absence of animal cells. The signal was then monitored in the sandwich complex formation-based manner on the label-free immunosensor

against time (Fig. S1, b). The binding signals obtained at different doses of TNF-α revealed that the minimum detection limit of the sensor was about < 1.25 ng/mL (see the standard curve in the inset). This indicated that the cytokine secreted from the host cells upon infection could be detected via label-free biosensing.

Performance characterization. The biosensor format shown in Fig. 1 was first characterized using a 200-μL culture volume towards analytical performance, particularly, the earliest detection time of infection. Among experimental conditions that may affect sensor performance, the stirring rate was selected as a primary controlling factor because it could significantly affect the interaction between TLRs of the host cells and PAMPs on the bacterium. The host cells (200 μL of 1×10^4 cells/mL) were initially immobilized on the culture container bottom surfaces and grown for 2 days. After removing the medium, the standard samples of *S. sonnei* as the infectious agent were then separately added concurrently with the transfer of the detection antibody to the cytokine. The immunosensor prepared by immobilizing the biotinylated rabbit antibody on the label-free optical fiber sensor via streptavidin-biotin linkage was placed within the solution. TNF-α production was monitored continuously within the Octet sensor system under different stirring rates, varied using the orbital shaker installed inside.

The biosensor revealed distinct response patterns according to the shaking speed, although the time-response sensorgram showed some drift during monitoring (Fig. 2). At high agitation (e.g., 600 rpm), the signals for the respective standard samples were increased from the baseline after different incubation times (Fig. 2, a). The response times were inversely proportional to the bacterium titer in a range > 1×10^3 CFU/mL and then reached a similar maximum intensity. On the other hand, the sensor response pattern at a slower agitation speed (e.g., 300 rpm) was significantly changed in the high titer range in which the maximal signal intensity was elevated as the infection dose was reduced, down to 1×10^4 CFU/mL (Fig. 2, b). The signal could even be measured for the sample containing the order of 10 CFU/mL, which was not detectable with the higher agitation (see the curve colored in yellow). Without shaking, both phenomena, signal amplification at lowered doses and sensitivity enhancement, were seen more clearly, and a sample containing about 10 CFU/mL bacterium was detected at < 10 h after inoculation (Fig. 2, c).

Rate-controlling steps. As mentioned earlier, cytokine secretion may be promoted mainly through the following double circuits: stimulation by the bacterial growth in an auto-catalytic manner [25] and autocrine/paracrine signaling via cytokine propagation [26]. Between the pathways, the rate-controlling step for the sensor response may vary depending on the stirring rate of the culture medium. When the stirring was vigorous (e.g., 600 rpm), the bacterium grown in the culture did not settle on the bottom of the container (process A-1 < A-2; Fig. 3) and the expansion was not retarded. The TNF-α secreted from the host cells (process B-1) may also be transferred away into the bulk solution rather than accumulated on the bottom surfaces to take part in signaling to neighboring cells (process B-2 < B-3). Thus, the cytokine production during the initial time period can be affected primarily by the bacterial growth, and abruptly increased as soon as the exponential growth phase is entered (see the left panel of Fig. 2 and below for details). This action alone of the bacterial stimulation circuit could consequently worsen the detection capability by more than 10^3 CFU/mL.

However, as the agitation was reduced or not used, as the extreme condition, the secreted cytokine could stay longer in the diffusion layer close to the bottom surfaces where the host cells were growing (process B-2 > B-3; Fig. 3). This will enable the cytokine to participate in various autocrine/paracrine signaling pathways mentioned earlier [26]. The bacterial expansion could also effectively promote cytokine production under such conditions because the bacterial particles settle down to the bottom. This will increase the local density, which expedites both the growth itself and infection of host cells. Because both circuits can now contribute the cytokine production in synergistic manner, the signal can eventually be detected even for the stimulation with a barely traceable bacterium (e.g., 10 CFU/mL bacterium; refer to the yellow curve in the right panel). The bacterial growth on the bottom layer, nevertheless, can cause local environmental change (e.g., high acidity) due to active metabolism of the growing bacterium, which will be discussed in the section below describing the medium volume effect on performance.

Establishment of Experimental Biosensor Models

Besides the agitation rate of culture medium, there could be other physical factors, such as volume of the medium, geometry of the container, and arrangement of the system components, that affect the analytical performance. In this initial study, we considered the

culture volume as a major performance-controlling factor. Because the bacterial growth usually lowered the pH of the culture medium, the effect of acidity, as a chemical factor, was considered further [27]. The pH distribution in the medium is certainly affected by physical parameters: the agitation speed and medium volume.

Medium volume. The medium volume was varied to test the effects on the detection capability. Although the system retaining a large culture volume (e.g., 200 μL) may be beneficial to supply enough nutrients to the host cells, secretory cytokine accumulation could be delayed until a certain level detectable by the sensor is reached. To alleviate this potential problem, we reduced the volume to a quarter of the conventional system (i.e., 50 μL). The ratio of the volume to the bottom surface area was 6.25 and 1.56 μL per mm^2 for the larger- and smaller-volume models, respectively (refer to Fig. S2 for details). The optical fiber sensor was placed close to the bottom of the container in both models (the mean distance: about 0.25 mm from the bottom). The liquid-air interfacial area was covered with mineral oil to prevent the culture medium from evaporation.

The real-time responses of the two biosensor models to standard samples were obtained separately under different stirring conditions and the performances were then compared. Time-response charts were reconstructed beforehand via baseline correction as presented in the Supplementary Information (refer to Fig. S3 for stepwise explanation). Among the revised response curves (Fig. S4), typical graphs were selected for non-agitated and highly agitated conditions, and then shown in an overlaid pattern (Fig. 4). When agitation of the culture medium was not used (Fig. 4, a), the 50-μL volume model showed a response much earlier than the 200-μL model, particularly for the sample containing a traceable bacterium (e.g., order of 10 CFU/mL; see the purple curves). However, the difference became smaller as the analyte titer was increased and eventually disappeared for the sample including a large quantity of target (e.g., order of 10^6 CFU/mL; see red curves). This pattern remained the same for the response curves obtained under stirring at 600 rpm although the response time to the same bacterial dose was consistently delayed compared with that not employing agitation (Fig. 4, b). It should be noted that the label-free sensing for TNF-α secreted from the cells was well matched regarding the response time with the ELISA outcome (refer to Fig. S5).

The results revealed that the response time of the sensor was more rapid in the smaller culture

volume, and also with less agitation, as described earlier. Because the 50-μL volume model retained a smaller volume based on the constant bottom surface area than the other, the cytokine secreted from the host cells could be concentrated earlier to a certain level detectable by the label-free sensor. In addition, the smaller-volume model showed a maximum signal intensity weaker than that of the larger model when the sample contained $> 10^3$ CFU/mL ~~bacteria~~ bacterium. In an extremely high titer range, $> 10^5$ CFU/mL, the signals even decreased significantly after reaching a maximum regardless of the stirring rate (see the red curves in Fig. 4). The volume change of the sensor could create an effect related to cytokine production and detection, as discussed in the next section.

Medium acidity. As the ~~bacteria~~ bacterium contained in a sample is grown in the culture, the metabolic activity continuously changes the chemical composition of the medium via substrate consumption and product formation. During the measurement period, the inoculated infectious agent may expand in an exponential pattern after a time lag, which will be shortened as the bacterial titer is elevated (Fig. S6). Such growth is usually accompanied by acidification of the culture medium [28], which was monitored by the mean pH change of the medium in parallel with the sensor response to TNF-α under the same conditions (Fig. 5). For sample including a low titer of bacterium (e.g., ~10^2 CFU/mL), the initial pH, 7.4, was constant during the monitoring period (Fig. 5, a). The sensor signal increased about 5 h after infection and then revealed saturation at about 9 h. When 10^4 CFU/mL ~~bacteria were~~ bacterium was inoculated, the medium pH began to decrease at about 3 h, reached pH 5.7 at 8 h, and was maintained constant thereafter (Fig. 5, b). The sensor also showed a response increase at the same time as the initial pH decrease, reaching a maximum at about 6 h, and then decreased continually. When the bacteria were augmented approximately 100 times again, the medium pH was decreased almost as soon as the ~~bacteria were~~ bacterium was inoculated (Fig. 5, c). Under such conditions, although the sensor signal could be measured relatively early, the signal was small and also sustained for about 3 h.

We have seen here that the sensor signal decrease could be caused by the chemical composition change of the culture medium such as acidification, which was intensified as the titer of ~~bacteria~~ bacterium in the sample was elevated. Because the bacterium *S. sonnei* had its own doubling time about 30 min [29], it entered into the exponential phase after a certain time lag, depending on the titer. The rapid metabolic increase at this phase may produce a

large quantity of products, including lactate [30], and could create a pH gradient in the axial direction from the bottom, particularly under non-agitated conditions. Such a local acidic environment near the bottom surface may result in two aspects related to the sensor signal: 1) the host cells may reduce cytokine secretion [31] and 2) the antigen-antibody complexes, which were formed beforehand, tend to dissociate [32]. The former could be more remarkable because the host cells may also undergo nutritional starvation and further hypoxia. The liquid-atmosphere interface was covered with mineral oil, as mentioned earlier. Hypoxia has been reported to reduce the secretion of LPS-induced TNF-α in mouse peritoneal macrophage cell lines (e.g., RAW 264.7, J774A.1, and PMJ-2R; [33]). The secreted TNF-α is also labile, with rapid degradation occurring in the extracellular environment [34]. Thus, as the bacterial titer is increased, the maximal magnitude of signal may be lowered and its duration of residual stay may also be shortened. Such phenomena ~~be~~ were more significant for a biosensor system using a smaller volume, i.e., the 50-μL model, (refer to Fig. S7 for comparison with the results for the 200-μL model) and less agitation.

Standard curves. We then determined the earliest response time and plotted it against the bacterial titer initially inoculated in the culture medium, which was repeated under different operating conditions (Fig. 6, a). The response time was determined as the earliest time corresponding to the signal obtained by multiplying the standard deviation of the default baseline by three. The triplicate measurements at each bacterial titer were averaged, and the mean response time was plotted against the titer initially inoculated in the culture medium. The response times obtained under different conditions were nearly identical at bacterial concentrations > 10^4 CFU/mL regardless of the stirring rate and medium volume used, but significantly diverged as the concentration was lowered. We estimated day-to-day variations using a formula, coefficient of variation (CV) = (standard deviation/average) × 100 [35], where the standard deviation was calculated for triplicate measurements under the same conditions at different days. The CVs were 28.6% for the 600 rpm & 200 μL system, 22.0% for the 0 rpm & 200 μL system, 22.5% for the 600 rpm & 50 μL system, and 19.5% for 0 rpm & 50 μL system. Such variations include all errors induced not only by the sensor system operation, but also by bacterial sample dilution.

We further characterized each system regarding performance-controlling factors (Fig. 6, b).

Among the conditions, the response of the non-stirred, small-volume system (a, 0 rpm, 50 μL) was the most rapid, particularly for bacterial infection < 10^4 CFU/mL. This may result from the possible synergistic stimulation of host cells via PAMPs-TLRs interaction and cytokine signaling, as described above (b, left bottom panel). On the other hand, local acidosis could occur on the bottom surfaces when the bacterial titer is > 10^4 CFU/mL. When either agitation was used (a, 600 rpm, 50 μL) or the volume was increased (a, 0 rpm, 200 μL), the response was delayed at the low range of bacterial titer. This may be caused by dilution of the secreted cytokine in each system via either agitation-induced convection in the former or extended molecular diffusion in the latter (b, left top or right bottom panels, respectively). For the sensor with high agitation and large volume (a, 600 rpm, 200 μL), the response was significantly retarded at the low range and samples with < 10^2 CFU/mL may even not be detected during the time span used. Under such conditions, the bacterial stimulation could act solely on host cell stimulation, as mentioned above, resulting in insensitive analysis especially for samples containing barely traceable ~~bacteria~~ bacterium (b, right top panel). This could eventually reveal the biphasic pattern of the standard curve, which, on the one hand, approached the lines for the other conditions in the high titer range of ~~bacteria~~ bacterium and, on the other, showed a very large response time in the lower concentration range (see the blue dotted curve in Fig. 6, a). According to the operating conditions selected, each plot can be used as the standard curve of the innate immune system-mimicking biosensor for quantifying the analyte in an unknown sample.

Application of the Non-stirred, Small-volume Model to Other Bacteria

As the non-stirred, small-volume system (0 rpm, 50 μL) showed enhanced performance regarding the response time, the model was applied to the analyses of other bacteria. Two additional species, *S. aureus* and *L. monocytogenes*, were selected as analytes potentially contaminating food [36]. After inoculation of each bacterium, the production of TNF-α was monitored inside the label-free sensor system, Octet Red, with respect to the incubation time, and the earliest detection time was then determined as the response of the sensor and the response time was plotted against the titer (Fig. 7, a). The data for the bacteria were linearly regressed by the least square method [37] to obtain an equation. Equations for the respective bacteria could be obtained with correlation coefficients (R^2) > 0.94, and they revealed

insignificantly different slopes ($P > 0.05$). The analytes could also be measured using the biosensor within about 8 h regardless of the bacterial species (7.6 h for *S. sonnei*, 8.2 h for *S. aureus*, and 7.9 h for *L. monocytogenes*) when the titer ≈ 50 CFU/mL (63±7.6 CFU/mL for *S. sonnei*, 53±8.2 CFU/mL for *S. aureus*, and 40±7.9 CFU/mL for *L. monocytogenes*).

The bacterial properties could differ towards stimulation of the immune system, such as virulence, mobility, and the presence of PAMPs [38]. As these can affect cytokine secretion, some variations in the sensor response may be inevitable according to the effects of diverse bacteria. Nevertheless, the slope of the response curves for different microorganisms appeared nearly identical, indicating that a major factor controlling the innate immune response could exist under the experimental conditions used. Among the variables, the growth rate of bacterium can be exemplified because the three microbes selected in this study had similar doubling times of about 3040 min [20]. Although it may be difficult to simply apply the same concept for all bacterial species, accumulation of data for pathogenic and non-pathogenic contaminants will come close to non-targeted detection. This concept may correspond to the non-selective cultivation of microbes in the microbiology area [39].

Real-sample Testing using the Novel Animal Cell-based Biosensor

Since the sensors revealed dose responses to bacterium in linear fashion ($R^2 > 0.94$) except for the high agitation and large volume system, the innate immune system-mimicked biosensing concept was further tested with real sample. To this end, we selected the non-stirred, small-volume system (0 rpm, 50 μL) as it relatively showed enhanced performance regarding the response time. Since milk is one of the extremely much consuming foods in the world, a product (Maeil Dairy; Seoul, Korea) was purchased to use for real sample testing. Three bacterium species, *S. aureus*, *L. moncytogens*, and *S. sonnei*, were also employed as significant analytes among those potentially contaminating the food [36]. *S. aureus* in milk can cause mastitis upon ingestion [40], *L. moncytogens* may result in a high lethality for unborn baby when a pregnant woman ingested the contaminated milk [41], and *S. sonnei* is a frequent microorganism found in raw milk [42]. The milk was first pretreated to reduce the fat content by mild centrifugation [43] and inoculated with defined titer of each bacterium. The inoculated, standard sample was mixed with the cell culture medium in the same volume ratio, which was then transferred into the container of the sensor system. When a bacterium is present in

the sample, it can grow and stimulate the animal cells in the synergistic manner [44] as mentioned above.

After loading a sample, the production of TNF-α was monitored inside the label-free sensor system, Octet Red, with respect to the incubation time and the earliest detection time was then determined as the response of the sensor. The same experiment was repeated at various concentrations of each bacterium and the response time was plotted against the titer (Figure 7, b). The data for the contaminant were linearly regressed by the least square method [37] to obtain an equation. The equations for the respective bacteria were able to be obtained with correlation coefficients (R^2) > 0.97, and they revealed insignificantly different slopes each other ($P > 0.05$). The analytes were able to be measured using the biosensor within about < 9.5 h regardless of the bacterial species when the titer ≈ 10^2 CFU/mL in sample.

The milk-sample testing results (Figure 7, b) were finally compared with those for the bacteria separately spiked in the culture medium as control (Figure 7, a). This revealed that the response time was prolonged in the presence of the real sample, which was more remarkable with the sample containing lower titer of each bacterium ($P < 0.001$). As milk as a popular food indeed contained many ingredients such as lipid, proteins, carbohydrate, mineral, and milk salts [45], the sample matrix could influence the sensor performance under the conditions used. The matrix can change the cell metabolism, and the nutrients such as oxygen and growth factors essential for the growth may also be limited by dilution. Therefore, the operating conditions described in this study would be needed to separately optimize for the respective real samples.

The non-targeted detection technique can be suited for automated analysis of bacterial contaminants which might be present in foods. As the technique employed a label-free sensor system commercially available, an early warning for the contamination could be feasible via real-time monitoring. Such ability for the bacterial analysis may substantially simplify food quality control process without using an additional sample pretreatment [46]. Furthermore, the non-targeted detection concept may also be used to screen foods containing bacteria exceeding a certain threshold number. For example, laboratory pasteurization count of milk and its fermented products [47] may be readily conducted as management practice using the same sensing technique. They can be checked in unattended manner whether normal bacteria

are contained < 100 CFU/mL. It should be stressed that, to eventually overcome threats and issues of food safety, tools enabling broad-spectrum screening for, for examples, bacteria, viruses, and fungi are needed in the first line of defense [3]. As the sensor developed in this study can be designed to respond to various cytokines secreted via innate immune system, it could further be used to screen variable microorganisms indicating potential contamination [48, 49].

Conclusions

Aspects of the innate immune system of animal cells (e.g., the RAW264.7 cell line) were used as a biosensor for the real-time monitoring of bacterial contamination so that sample testing could be carried out in an automated manner without handling. A cytokine, TNF-α, secreted from the bacterially infected cells in the cell culture container, such as a microtiter plate, could be monitored continuously using a label-free immunosensor. In the initial study for optimization, the volume and agitated state of the culture medium were selected as factors primarily controlling the earliest response time of the sensor. As the volume was increased or the agitation became vigorous, the response was retarded due to diffusive or enforced dilution of the secreted cytokines, which play a crucial role in autocrine/paracrine signaling. Among those tested, a biosensor model containing 50 μL medium and using no agitation was applied to the detection of different bacterial species (e.g., *S. aureus*, *L. moncytogens*, and *S. sonnei*), which enabled us to monitor bacterial contamination within the working time period. When the biosensor was further tested with real sample (e.g., milk), the initial response times for the various bacteria were consistent although they were somewhat prolonged due to sample matrix effect. Because the infectious stimulation is initiated by the interaction of PAMPs and pattern recognition receptors [50], the concept could be applied in principle to analyses of non-targeted microbial species such as bacteria, viruses, and fungi, which may contaminate [48, 49, 51], for example, foods, the environment, or even human blood. We are developing a novel sensor model minimizing the sample matrix effect, which will be particularly beneficial for analyzing samples containing a barely traceable microorganism.

Acknowledgements

This study was supported by the Korea Research Council of Fundamental Science & Technology (KRCF; Project in the year 2013). This work was also supported by the BK21 plus program of the Ministry of Education, Korea.

References

1. P. S. Mead, L. Slutsker, V. Dietz, L. F. McCaig, J. S. Bresee, C. Shapiro, P. M. Griffin and R. V. Tauxe, *Journal of Environmental Health*, 2000, 62.
2. G. Reid, J. A. Younes, H. C. Van der Mei, G. B. Gloor, R. Knight and H. J. Busscher, *Nature Reviews Microbiology*, 2010, 9, 27-38.
3. P. Banerjee and A. K. Bhunia, *Trends in biotechnology*, 2009, 27, 179-188.
4. E. C. Alocilja and S. M. Radke, *Biosensors and Bioelectronics*, 2003, 18, 841-846.
5. L. Manning, R. Baines and S. Chadd, *British Food Journal*, 2005, 107, 225-245.
6. Y.-H. Kim, J.-S. Park and H.-I. Jung, *Sensors and Actuators B: Chemical*, 2009, 138, 270-277.
7. T. K. Ling, Z. Liu and A. F. Cheng, *Journal of clinical microbiology*, 2003, 41, 4705-4707.
8. R. K. Saiki, T. L. Bugawan, G. T. Horn, K. B. Mullis and H. A. Erlich, *Nature*, 1986, 324, 163-166.
9. D. Dance, V. Wuthiekanun, P. Naigowit and N. White, *Journal of clinical pathology*, 1989, 42, 645-648.
10. M. Kubista, J. M. Andrade, M. Bengtsson, A. Forootan, J. Jonák, K. Lind, R. Sindelka, R. Sjöback, B. Sjögreen and L. Strömbom, *Molecular aspects of medicine*, 2006, 27, 95-125.
11. D. Klein, *Trends in molecular medicine*, 2002, 8, 257-260.
12. C. Yang, Y. Jiang, K. Huang, C. Zhu and Y. Yin, *FEMS Immunology & Medical Microbiology*, 2003, 38, 265-271.
13. R. Medzhitov and C. A. Janeway Jr, *Current opinion in immunology*, 1997, 9, 4-9.
14. A. Aderem and R. J. Ulevitch, *Nature*, 2000, 406, 782-787.
15. D. M. Underhill, *European journal of immunology*, 2003, 33, 1767-1775.
16. M. Lappas, M. Permezel, H. M. Georgiou and G. E. Rice, *Biology of Reproduction*, 2002, 67, 668-673.
17. R. Vézina Audette, A. Lavoie-Lamoureux, J.-P. Lavoie and S. Laverty, *Osteoarthritis and Cartilage*, 2013, 21, 1116-1124.
18. D. Venkatesh, T. Ernandez, F. Rosetti, I. Batal, X. Cullere, F. W. Luscinskas, Y. Zhang, G. Stavrakis, G. García-Cardeña and B. H. Horwitz, *Immunity*, 2013, 38, 1025-1037.
19. A. Yarilina, K.-H. Park-Min, T. Antoniv, X. Hu and L. B. Ivashkiv, *Nature*

immunology, 2008, 9, 378-387.

20. I.-H. Cho, J.-W. Jeon, S.-H. Paek, D.-H. Kim, H.-S. Shin, U.-H. Ha, S.-K. Seo and S.-H. Paek, *Analytical chemistry*, 2012, 84, 9713-9720.
21. R. Farahi, A. Passian, L. Tetard and T. Thundat, *ACS nano*, 2012, 6, 4548-4556.
22. K. Huttunen, A. Hyvärinen, A. Nevalainen, H. Komulainen and M.-R. Hirvonen, *Environmental Health Perspectives*, 2002, 111, 85-92.
23. J. Cohen, *Nature*, 2002, 420, 885-891.
24. A. García-Fulgueiras, S. Sánchez, J. Guillén, B. Marsilla, A. Aladueña and C. Navarro, *European journal of epidemiology*, 2001, 17, 533-538.
25. H. Martínez, J. Sánchez, J.-M. Cruz, G. Ayala, M. Rivera and T. Buhse, *The Scientific World Journal*, 2014, 2014.
26. L. Vitkovic, J. Konsman, J. Bockaert, R. Dantzer, V. Homburger and C. Jacque, *Molecular psychiatry*, 2000, 5, 604-615.
27. P. D. Cotter and C. Hill, *Microbiology and Molecular Biology Reviews*, 2003, 67, 429-453.
28. S. D. Patel, E. T. Papoutsakis, J. N. Winter and W. M. Miller, *Biotechnology progress*, 2000, 16, 885-892.
29. J. Mitobe, T. Morita-Ishihara, A. Ishihama and H. Watanabe, *BMC microbiology*, 2009, 9, 110.
30. D. G. Barceloux, *Medical toxicology of natural substances: foods, fungi, medicinal herbs, plants, and venomous animals*, John Wiley & Sons, 2008.
31. T. A. Heming, D. M. Tuazon, S. K. DAVÉ, A. K. Chopra, J. W. Peterson and A. Bidani, *Clinical Science*, 2001, 100, 259-266.
32. R. Reverberi and L. Reverberi, *Blood Transfusion*, 2007, 5, 227.
33. N. Lahat, M. A. Rahat, A. Kinarty, L. Weiss-Cerem, S. Pinchevski and H. Bitterman, *American Journal of Physiology-Cell Physiology*, 2008, 295, C2-C12.
34. G. Ozbey, R. Gorczynski and N. Erin, *European Cytokine Network*, 2014, 25, 30-34.
35. L. H. Koopmans, D. B. Owen and J. Rosenblatt, *Biometrika*, 1964, 25-32.
36. R. F. Wang, W. W. Cao and C. Cerniglia, *Journal of Applied Microbiology*, 1997, 83, 727-736.
37. G. Golub, *Numerische Mathematik*, 1965, 7, 206-216.
38. J. Wilson, M. Schurr, C. LeBlanc, R. Ramamurthy, K. Buchanan and C. Nickerson, *Postgraduate medical journal*, 2002, 78, 216-224.

39. J. Slots, *Oral microbiology and immunology*, 1986, 1, 48-55.
40. Ö. Akineden, C. Annemüller, A. Hassan, C. Lämmler, W. Wolter and M. Zschöck, *Clinical and diagnostic laboratory immunology*, 2001, 8, 959-964.
41. C. B. Dalton, C. C. Austin, J. Sobel, P. S. Hayes, W. F. Bibb, L. M. Graves, B. Swaminathan, M. E. Proctor and P. M. Griffin, *New England Journal of Medicine*, 1997, 336, 100-106.
42. J. M. Leedom, *Clinical infectious diseases*, 2006, 43, 610-615.
43. D. Peedel and T. Rinken, *Analytical Methods*, 2014, 6, 2642-2647.
44. J.-W. Jeon, U.-H. Ha and S.-H. Paek, *PloS one*, 2014, 9, e105212.
45. M. Playne, L. Bennett and G. Smithers, *Australian Journal of Dairy Technology*, 2003, 58, 242-264.
46. S.-M. Seo, I.-H. Cho, J.-H. Kim, J.-W. Jeon, E.-G. Oh, H.-S. Yu, S.-B. Shin, H.-J. Lee and S.-H. Paek, *Bull. Korean Chem. Soc*, 2009, 30, 2993.
47. B. Jayarao, S. Pillai, A. Sawant, D. Wolfgang and N. Hegde, *Journal of Dairy Science*, 2004, 87, 3561-3573.
48. E. Tengstrand, J. Rosén, K.-E. Hellenäs and K. M. Åberg, *Analytical and bioanalytical chemistry*, 2013, 405, 1237-1243.
49. G. Zuccheri and N. Asproulis, *Detection of pathogens in water using micro and nano-technology*, IWA publishing, 2012.
50. J.-W. Jeon, I.-H. Cho, U.-H. Ha, S.-K. Seo and S.-H. Paek, *Scientific reports*, 2014, 4.
51. O. Lazcka, F. Campo and F. X. Munoz, *Biosensors and Bioelectronics*, 2007, 22, 1205-1217.

Figure Legends

Fig. 1 Schematic representation of the innate immune response-mimicking biosensing for microorganisms. The biosensing system can be constructed by combining an animal cell culture that retains the cells (e.g., macrophage cell line; RAW264.7) grown on the surfaces of a 96-well microtiter plate with an immunosensor, which includes an antibody, specifically recognizing a cytokine (e.g., TNF-α), immobilized on the tip of an optical fiber sensor. When a bacterium is present in the sample medium, it can infect the host cells (a) and secrete cytokines as proinflammatory mediators after a certain time period (b). The cytokine molecules are then captured by the antibody on the sensor tip (c), which produces a mass-sensitive signal in a label-free manner.

Fig. 2 Typical real-time responses of the cell-based biosensor (200-μL culture volume) to *S. sonnei* in samples under various stirring rates. The RAW264.7 cells were stably cultured on the container surfaces and, after adding the standard sample of *S. sonnei*, the TNF-α secretion was immediately monitored in real time under different stirring conditions (0 to 600 rpm). The cytokine was measured by a sandwich immunoassay using a label-free sensor with the capture antibody on the tip surfaces (Fig. 1). As the stirring rate was reduced, the signal at lowered concentrations of the bacterium appeared to increase significantly and, therefore, the sensitivity was enhanced.

Fig. 3 Effect of culture medium agitation on stimulation of the innate immune system of the host cells. Because the bacterial binding to the TLRs is the initial step (process A-1) for cytokine (e.g., TNF-α) production (B-1), agitation may disturb the interaction by taking the bacterium away from the bottom surfaces (A-2). The cytokine secreted from the cells could have two ways of propagation to neighboring host cells (B-2) or transfer to the bulk solution (B-3), also depending on the agitated condition.

Fig. 4 Typical, revised real-time responses of the cell-based biosensor models, containing different culture volumes (50 or 200 μL), to the *S. sonnei* titers under different agitation conditions. The RAW264.7 cells were stably cultured on the container surfaces and, after adding the standard sample of *S. sonnei* indicated, TNF-α secretion was immediately

monitored in real time. Regardless of the stirring rate, the biosensor using the smaller volume showed earlier response times, particularly for samples containing bacteria < about 10^3 CFU/mL. However, the difference became negligible when the sample contained the analyte > 10^5 CFU/mL. Refer to the text for details.

Fig. 5 Monitoring of mean pH of the culture medium (marked) and TNF-α (red-colored) under the same conditions using the 50 μL-holding model without agitation. The pH was measured discretely while the cytokine was monitored continuously in real time. The initial pH, 7.4, was maintained constant for a sample containing a low concentration of bacteria (a), but decreased to a larger degree at an earlier time as the sample contained a higher titer of the bacteria (b and c). Such chemical changes to the medium could result in the cytokine signal being smaller and also staying shorter. Refer to the text for detailed discussion.

Fig. 6 Standard curves for the response time versus *S. sonnei* concentration under various operating conditions, which may vary the performance-controlling factor. Although the response times were not much different for bacteria > 10^4 CFU/mL, they diverged significantly in the lower concentrations. According to the conditions used, the response time was ranked in the following order (a): 0 rpm, 50 μL < 600 rpm, 50 μL or 0 rpm, 200 μL < 600 rpm, 200 μL. Such variation could be determined by the host cell stimulation mainly via cytokine signaling (b): high, intermediate, or low, respectively, for the three cases. These experiments were conducted in triplication. Refer to the text for details.

Figure 7. Application of the animal cell-based biosensor (0 rpm, 50 μL) to the detection of various bacteria present in the culture medium as control (a) or a food sample, milk (b). Two Gram-positive bacteria, *S. aureus* and *L. monocytogenes*, and a Gram-negative bacterium, *S. sonnei*, were selected as potential pathogenic food contaminants and separately inoculated in each sample. The sample was mixed with the culture medium in the same volume ratio and then added into the cell culture container. After placing the sensor within the system, Octet Red, the signal was measured with respect to the incubation time, during which the earliest detection time was determined as the response. The identical experiment was repeated at different bacterial titers, and the response time was plotted against the titer. The data for the respective bacterium were linearly regressed with correlation coefficients (R^2) > 0.97. Comparison between the two results for different samples shown in a and b, respectively, was

indicated significance ($P < 0.05$). The same measurement was repeated three times.

Figures

Fig. 1

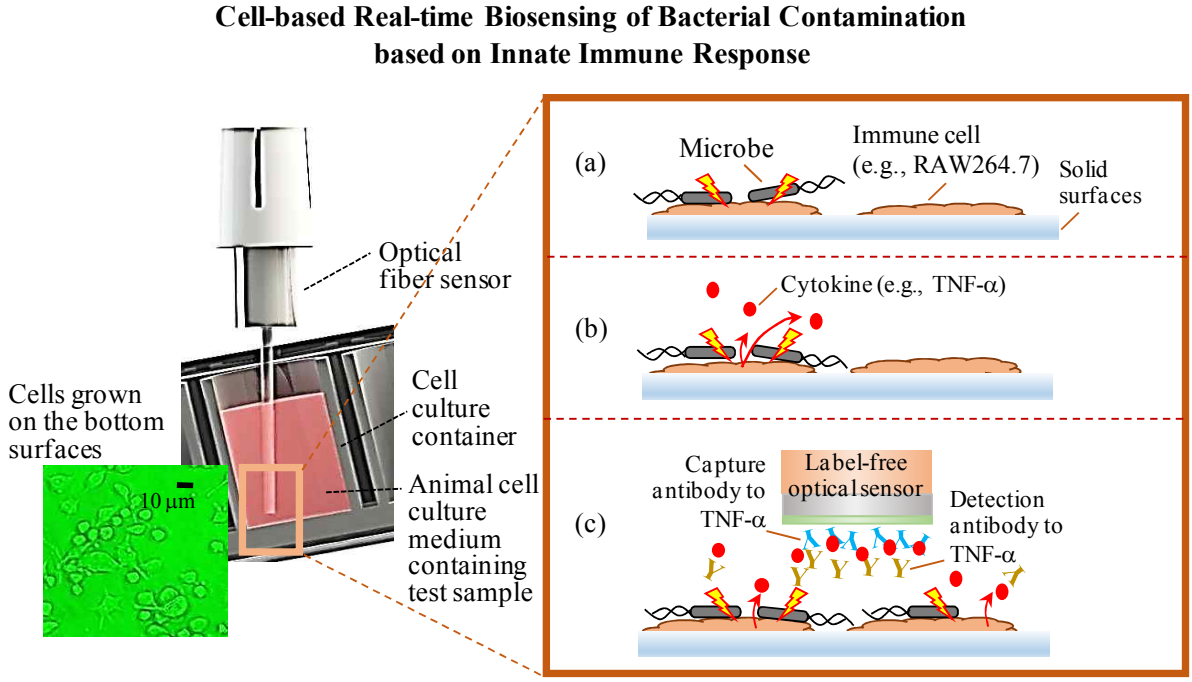

Fig. 2

(a) Real-time dose responses under stirring rate = 600 rpm

(b) Real-time dose responses under stirring rate = 300 rpm

(c) Real-time dose responses under stirring rate = 0 rpm

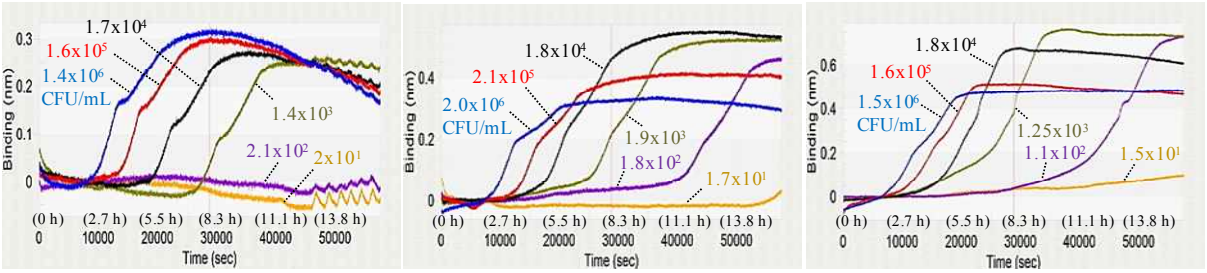

Fig. 3

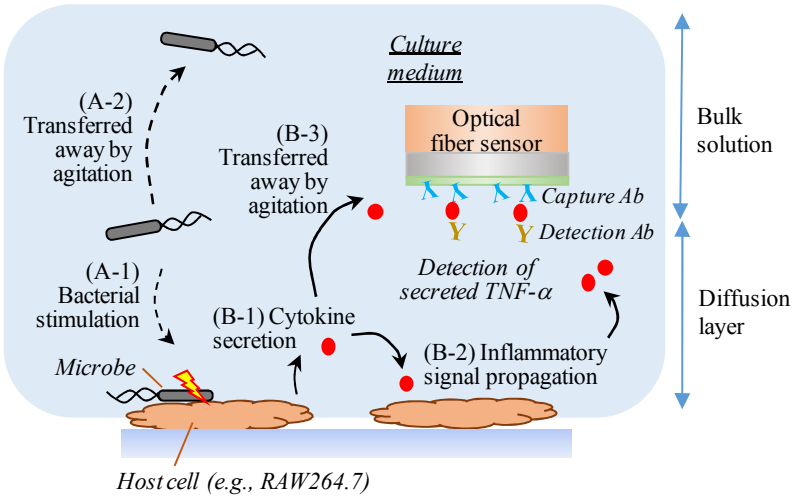

Fig. 4

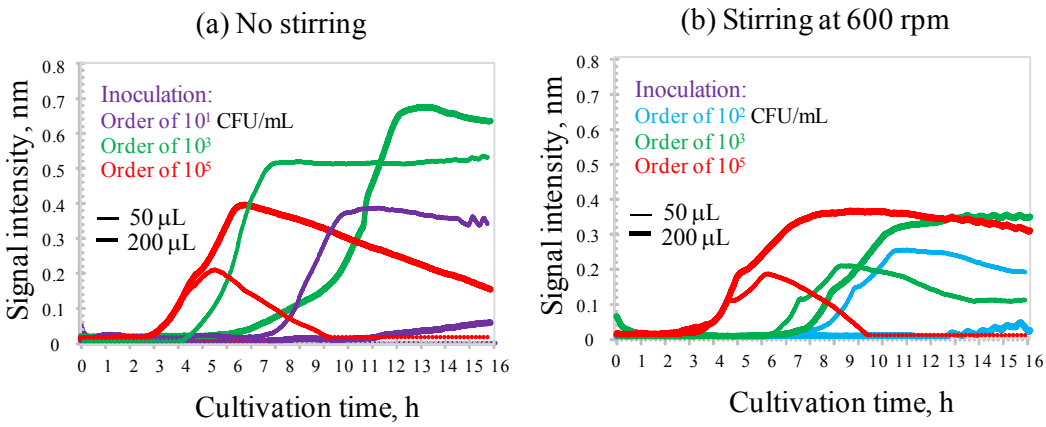

Fig. 5

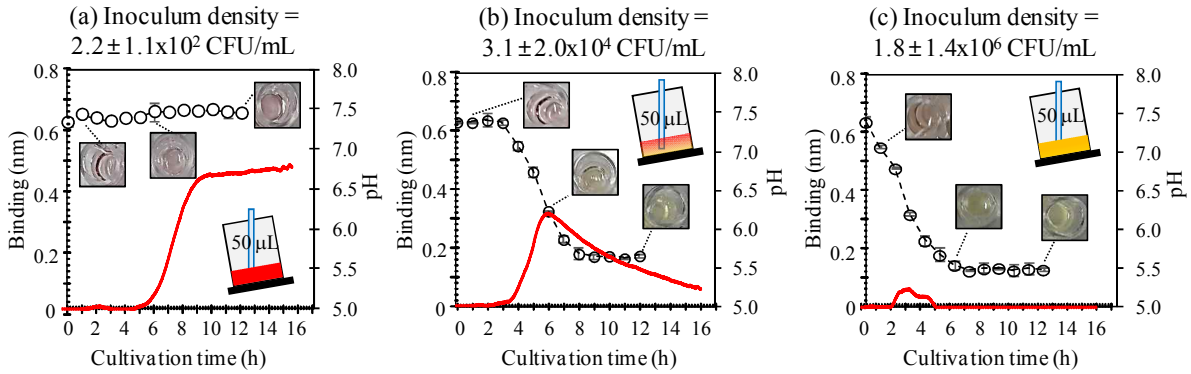

Fig. 6

(a) Standard curves of the biosensor for *S. sonnei*

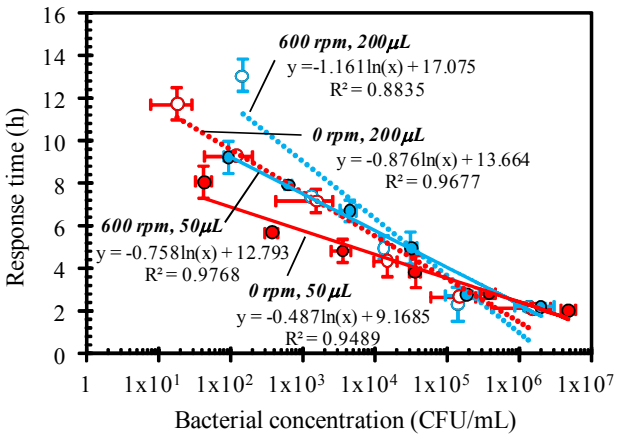

(b) Characterization of factors determining the host cell stimulation

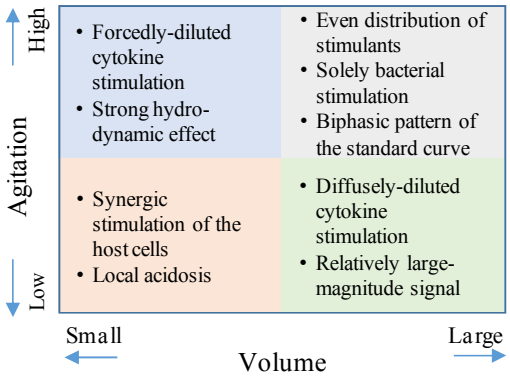

Fig. 7